HHS Public Access

Author manuscript

Ann Surg Oncol. Author manuscript; available in PMC 2014 October 01.

Published in final edited form as:

Ann Surg Oncol. 2013 October ; 20(11): 3685–3693. doi:10.1245/s10434-012-2434-z.

Three-dimensional Optical Coherence Tomography for Optical Biopsy of Lymph Nodes and Assessment of Metastatic Disease

Renu John, PhD[1], **Steven G. Adie, PhD**[1], **Eric J. Chaney, BS**[1], **Marina Marjanovic, PhD**[1], **Krishnarao V. Tangella, MD**[2], and **Stephen A. Boppart, MD, PhD**[1,3]

[1]Beckman Institute for Advanced Science and Technology, University of Illinois at Urbana-Champaign, Urbana, IL

[2]Department of Pathology, College of Medicine, University of Illinois at Urbana-Champaign, Urbana, IL

[3]Departments of Bioengineering, Electrical and Computer Engineering, and Medicine, University of Illinois at Urbana-Champaign, Urbana, IL

Abstract

Background—Numerous techniques have been developed for localizing lymph nodes before surgical resection and for their histological assessment. Nondestructive high-resolution transcapsule optical imaging of lymph nodes offers the potential for in situ assessment of metastatic involvement, potentially during surgical procedures.

Methods—Three-dimensional optical coherence tomography (3-D OCT) was used for imaging and assessing resected popliteal lymph nodes from a preclinical rat metastatic tumor model over a 9-day time-course study after tumor induction. The spectral-domain OCT system utilized a center wavelength of 800 nm, provided axial and transverse resolutions of 3 and 12 μm, respectively, and performed imaging at 10,000 axial scans per second.

Results—OCT is capable of providing high-resolution labelfree images of intact lymph node microstructure based on intrinsic optical scattering properties with penetration depths of ~1–2 mm. The results demonstrate that OCT is capable of differentiating normal, reactive, and metastatic lymph nodes based on microstructural changes. The optical scattering and structural changes revealed by OCT from day 3 to day 9 after the injection of tumor cells into the lymphatic system correlate with inflammatory and immunological changes observed in the capsule, precortical regions, follicles, and germination centers found during histopathology.

Conclusions—We report for the first time a longitudinal study of 3-D transcapsule OCT imaging of intact lymph nodes demonstrating microstructural changes during metastatic infiltration. These results demonstrate the potential of OCT as a technique for intraoperative, real-time in situ 3-D optical biopsy of lymph nodes for the intraoperative staging of cancer.

Lymph nodes are highly specialized and vital immunological organs in the lymphatic system. They serve to filter and identify foreign particles and antigens to elicit an

S. A. Boppart, MD, PhD, boppart@illinois.edu.

immunologic response. The assessment and status of lymph nodes serves as an important indicator for metastatic spread of cancer, for staging the extent of the disease to determine therapeutic regimens, and for making a prognosis. Lymph nodes have a well-defined and dynamically responsive microstructure with an outer capsule, subcapsular sinus, cortex containing follicles and B cells, paracortex containing T cells, medullary sinuses, medullary cords, and hilus.[1] A proper evaluation of their gross and microscopic features reflects the pathological condition of those parts of the body that drain to the respective nodes. Currently, the assessment of lymph nodes in surgical oncology is routinely performed postoperatively by a histopathologist, primarily to determine if there has been metastatic involvement.

Current clinical imaging modalities including X-ray, MRI, CT, ultrasound, and PET are considered as options for noninvasive in situ imaging of lymph nodes, with each having various advantages and disadvantages. However, the resolution of these modalities largely only permits the assessment of node size, and other than PET, the assessment of lymph nodes using these modalities mostly relies on lymph node anatomy rather than function and physiology.[2] The sizes of lymph nodes, along with some information about morphology, have been the primary differentiating criteria for nodal staging with these imaging modalities. However, this approach has low accuracy and cannot be used to reliably distinguish between node enlargement due to cancer or to inflammation.[3,4] Also, the imaging resolution of these modalities is not sufficient to reveal lymph node microstructure and perform an in vivo assessment of any lymph node metastasis involving partial or microscopic infiltration of tumor cells, rather than only gross morphology. The use of contrast agents such as gadolinium and iron oxide nanoparticles in MRI has been explored for assessing alterations in lymph node microcirculation such as flow characteristics, blood volume, microvascular permeability, and increased fractional volume of the extravascular extracellular space.[5–9] However, these contrast agents take an extended period of time to distribute through the lymphatic system. None of the above mentioned methodologies currently enable the intraoperative assessment of lymph node status.

Several techniques have been developed to localize lymph nodes, primarily sentinel lymph nodes, before resection during cancer surgery. These have traditionally included the use of a radiotracer (technetium-99 m) or dye (methylene blue, Lymphazurin) and the use of near-infrared optical dyes coupled with intraoperative fluorescence imaging systems are currently being investigated.[10–13] All of these methods, however, rely solely on identifying and localizing lymph nodes, rather than enabling an assessment of the lymph node status (normal, reactive, metastatic). Other optical techniques such as light and confocal microscopy in the operating room have been used to visualize lymph node specimens or touch preparations, but have required the resection and ex vivo bisection of the nodes to expose the microarchitecture for high-resolution imaging, and are not practical for in situ assessment.[14,15]

Optical coherence tomography (OCT) is an emerging in vivo imaging modality with typical axial and transverse resolutions of 1–5 μm and 10–15 μm, respectively, and the capability of providing real-time microscopic images up to 2 mm beneath the tissue surface, even in highly scattering tissues.[16–18] OCT has shown potential for use in high-resolution surgical

guidance.[19–21] In addition, OCT has been previously used to image breast cancer tumor margins intraoperatively in human subjects, and other studies have shown the potential of OCT for imaging morphological features related to cancer metastasis and intraoperatively identifying metastatic nodes.[22–25] In one study ex vivo human axillary lymph nodes were bisected to cut open the capsule structure and expose inner structures for imaging, while other work has focused on transcapsule imaging.[23–25] Though preliminary reports have been promising, no systematic studies have been performed to assess the capability of OCT for imaging changes that occur in the time-dependent progression of lymph node metastases. Identifying OCT image-based microscopic structural changes that enable lymph node assessment and classification as normal, reactive, or metastatic would aid the clinical staging of the disease, with the potential for assessment and staging to occur in real-time, during surgical procedures.

Our primary aim for this study was to analyze the microstructural and pathological changes in intact lymph nodes at different stages of metastatic involvement using 3-D OCT, which is not possible from discrete human specimens in unpredictable or uncontrolled pathological stages. To accomplish this, we utilize a preclinical rat tumor metastases model to perform a controlled longitudinal time-dependent study of the progression of lymph node metastases. We performed transcapsule 3-D OCT imaging of physically intact popliteal lymph nodes resected from this rat tumor model, rather than bisecting nodes to expose internal microstructure. The metastatic lymph nodes were induced in this rat tumor metastasis model by injecting tumor cells into the hind leg foot pad of the animals, and popliteal lymph nodes were imaged ex vivo at day 3 to day 9 time points after injection. The 3-D OCT images were analyzed and compared with images from popliteal lymph nodes from control animals. Corresponding histopathological analysis was performed on all specimens in parallel. Our previous results have suggested that 3-D OCT could have significant potential for identifying early changes in lymph node morphology related to metastatic invasion based on the differences in the optical scattering properties of the tissue.[23,25] This study is designed to explore if OCT can be used to image and assess lymph node status at various stages of metastatic involvement or infiltration, thus providing an atlas of optical image biomarkers that can be used in the future to compare with the real-time feedback and diagnostic image information acquired during surgical interventions.

MATERIALS AND METHODS

Animal Model

Experiments were performed in compliance with an experimental protocol approved by the Institutional Animal Care and Use Committee at the University of Illinois at Urbana-Champaign. Inbred Fischer F344 female rats (n = 10, 32 days old) (Harlan, Indianapolis, IN) were used in this study, providing two rats (two popliteal lymph nodes) per longitudinal time point. To induce metastasizing tumors and metastatic lymph nodes, tumor cells were injected into one hind-limb foot pad as previously described.[26] Briefly, rat mammary tumor cells (13762 MAT B III, ATCC #CRL-1666, ~5 9 $\times 10^6$ cells per animal) were injected into the left footpad (day 0) to form tumors that would develop in the footpad and metastasize to the popliteal lymph nodes through the lymphatic drainage network of the foot and leg.

Results were referenced to control rats that received only saline injections into the footpad. The popliteal lymph nodes from the animals injected with tumor cells were imaged ex vivo using 3-D OCT on days 3, 5, 7, and 9 after injection. These time points were selected on the basis of a pilot study (3 rats injected with 5×10^5 tumor cells per animal) which showed that advanced metastatic disease was present in the lymph nodes on days 12 and 13 after injection. Before imaging, the animals were anesthetized by intraperitoneal injection with a combination of ketamine (100 mg/kg) and xylazine (10 mg/kg), and a 1 % isosulfan blue solution (Lymphazurin; U.S. Surgical Corp., Norwalk, CT) was injected into the footpad tumor site and allowed to circulate for 5 min to map out the lymphatic drainage system. Animals were sacrificed, and a portion of the footpad tumor along with right and left popliteal lymph nodes were removed and imaged by 3-D OCT. Histopathological evaluation of the popliteal lymph nodes was carried out after OCT imaging.

OCT Imaging

A spectral-domain OCT system was used for ex vivo imaging of lymph nodes. A femtosecond titanium:sapphire laser (KMLabs, Inc.) with a bandwidth of 110 nm centered at a wavelength of 800 nm providing an axial resolution of ~3 μm was used as the light source. The laser was pumped by a frequency-doubled Nd:YVO_4 laser (Coherent Inc.) with 4.5 W of 532 nm light. The broadband light was launched into a single-mode fiber interferometer which was divided into the sample arm and a stationary reference arm. The sample arm beam was steered using galvanometermounted mirrors for 3-D OCT imaging. The samples were imaged with an achromatic lens with a focal length of 30 mm, producing a transverse resolution of ~12 μm. The power in the sample arm was 10 mW. The interference of the reference and sample beams was measured with a spectrometer composed of a grating, imaging lens, and line camera (Piranha 2, Dalsa Inc.) with a capability of 33 kHz line acquisition rates. The spectrometer resolution was designed to provide an optical imaging depth of 2 mm.

Two-dimensional B-mode imaging of the specimens, followed by transverse scanning in the third (y) direction with spacing of 10 μm using galvanometer mirrors, was performed to achieve 3-D reconstructions of the lymph nodes. Images were acquired at an axial scan rate of 10 kHz and a camera exposure time of 90 μs, with an image capture time of 0.4 s per cross-sectional B-mode image. A typical 3-D OCT data set contained 300 B-mode images in each volume. Significantly faster volumetric imaging is possible with recent advances in optical sources for OCT, enabling these 3-D volumes to be acquired in <1 s.[27,28] En face images were computationally extracted from the 3-D volumes to illustrate lymph node features with resolution that was uniform in the *x*–*y* plane (~12 μm), in contrast to the cross-sectional (*x*–*z*) OCT images that had different resolutions in each direction (~12 μm and ~3 μm, respectively). It should be noted that 3-D OCT was performed transcapsule, from resected but physically intact lymph nodes. This is in contrast to many other optical imaging studies where lymph nodes are bisected to expose inner structures for imaging. The transcapsule approach is intended to validate the potential for using 3-D OCT on in situ lymph nodes in the future.

The portable OCT system that would be used during surgery would be contained in a small cart and easily maneuvered into the operating room for imaging during procedures. OCT imaging would be performed in situ by a surgeon using a handheld surgical probe, or ex vivo by trained OR staff on any excised specimens. Real-time OCT images from the portable system would allow a surgeon to intraoperatively determine whether lymph nodes contain metastatic disease.

Histopathology Protocol

The lymph nodes were fixed in formalin, paraffin embedded, and sectioned at a thickness of 10 μm. The tissue sections were stained with hematoxylin and eosin. The histology slides were digitized using a light microscope (Carl Zeiss, Germany), and auto-stitched together (Adobe Photoshop CS4) to provide a single montage for illustration. The hematoxylin and eosin–stained histology slides were evaluated by a board-certified clinical pathologist and classified as normal, reactive, or metastatic. The histological processing and analysis were performed in a blinded fashion, without knowing the history of the animals.

RESULTS

The OCT images of all control lymph nodes clearly showed normal structure (Figs. 1, 2) featuring an intact capsule and follicular structures that were distinguishable from the background cortex on the basis of their spheroidal pattern of optical scattering. In addition, the outer adipose tissue, capsule, and precortical regions were distinct in the OCTimages. Figure 1 presents a representative example of a 3-D OCT reconstruction of a normal lymph node, along with the cross-sectional (*y*–*z* and *x*–z) and *en face* (*x*–*y*) images.*En face* images showed more useful detail when compared to cross-sectional OCT images. This may be due to the uniform resolution available in the *x*–*y* plane, as compared to crosssectional images which had different resolutions along the depth and transverse axes. The features observed in the OCT images correlate well with the corresponding histological sections, and both served as a reference to identify architectural changes and stage metastatic infiltration in the images from the other animals.

The observed lymph node capsular structure becomes less distinct in the OCT and histology images of the lymph nodes on day 3 after the injection of tumor cells (Fig. 3). Gross macroscopic inspection revealed mild inflammation of the lymph nodes. The histology verifies an infiltration of macrophages, but no clear evidence of anaplasia indicating the presence of tumor cells in the subcapsular space was found. There was also a mild increase in scattering from the follicles in the OCT images.

Lymph node images on day 5 after injection of tumor cells showed a disappearance and disruption of the capsule, and the appearance of a new heterogeneous low-scattering layer in the subcapsular space (Fig. 4). In these images, all the follicles are clearly visible and highly scattering. Histological findings suggest infiltration of tumor cells and macrophages from the subcapsular space into the precortical regions, which is clear evidence of early metastasis. The germination centers became more reactive, resulting in increased scattering in the OCT images.

The OCT images of lymph nodes from day 7 rats show that the newlow-scattering subcapsular layer thickens and extends into the deeper regions of the node (Fig. 5b, position of the cross section is indicated by a green horizontal line in Fig. 5a). The follicles are no longer visible, indicating a disruption of the follicular structure, and an increase of optical scattering from regions deeper in the lymph nodes. The histology results from this time point correlate very well with theOCT findings (Fig. 5d). Lymph nodes were enlarged with aggregates of macrophages and tumor cells migrating from the subcapsular to paracortical regions (Fig. 5e). Sheets ofmetastatic cells and macrophages infiltrating into the precortical regions of the lymph node correlate with the low scattering regions onOCT. The thickness of this layer increases as the tumor cells proliferate, eventually spreading throughout the lymph node. However, another area fromthe day 7 rat (Fig. 5c; position of the cross section is indicated by a yellow horizontal line in Fig. 5a), show only inflammatory changes resulting in low scattering inner regions with surrounding highly scattering cells. The corresponding histological observations report aggregates of macrophages in the cortical and paracortical regions, with compression of normal lymphoid tissue to the periphery and no tumor cells present (Fig. 5f).

The lymph nodes from the day 9 after injection rats clearly show uniform high-scattering regions in the OCT images from the disruption of normal lymph node structure (Fig. 6), indicating a metastatic tumor-filled node. Histology supports these observations, reporting total effacement of the nodal architecture, including the cortical, paracortical, and medullary regions, with a metastatic neoplastic mass of cells. This result is consistent with OCT and histology results from the pilot study, which showed complete metastatic invasion by day 12 and 13 after injection.

DISCUSSION

This controlled study demonstrated that OCT is capable of identifying early changes in lymph node morphology which are all well correlated to the corresponding histopathological findings. These include: larger follicles in reactive lymph nodes showing an inflammatory response, presence or disappearance of the outer capsule structure, appearance of a low scattering layer along the outer edges of the subcapsular space (indicating infiltration of macrophages), and infiltration of tumor cells in this region.

Three-dimensional OCT imaging of lymph nodes at varying stages of metastatic involvement show imagebased optical scattering features that strongly correlate with histological findings. These results suggest that 3-D OCT has potential for future in situ analysis of lymph nodes for staging cancer metastases intraoperatively. This OCT study was performed in a well-characterized preclinical animal model for lymph node metastases. The use of this animal model enabled the investigation of optical scattering and OCT image changes at various time-points and stages during metastatic involvement in a way that would not have be possible in human patients.

In this study, we performed ex vivo transcapsule 3-D OCT imaging of physically intact popliteal lymph nodes to observe their time-dependent changes from normal to grossly metastatic. Before this study, only images of discrete changes in time in various specimens

were available, which could not fully track longitudinally the time-dependent optical changes that occur during metastases.[24,25]

The OCT images presented here clearly show the microscopic lymph node structure. The optical scattering and structural changes revealed by 3-D OCT from day 3 to day 9 after injection of tumor cells into the lymphatic system clearly indicate the progressive involvement of metastatic tumor cells and new tumor growth in the lymph nodes. The results also correlate well with the inflammatory and immunological changes observed in the capsule, precortical regions, follicles, and germination centers observed in the histopathological sections.

Identification of microstructural changes in OCT images corresponding to various stages of infiltration and more importantly, optical differences between normal nonreactive, reactive, and metastatic nodes was feasible using this controlled tumor metastasis model. Further work is required to investigate the biological variability between lymph nodes at any given time point. Ongoing studies are exploring the potential of high resolution OCT for detecting early micrometastasis of sizes <100 μm within the intact lymph nodes, which has clinical significance.[29] In current clinical practice, the sentinel lymph node or nodes associated with the tumor site are removed for postoperative histological assessment and staging of the cancer. Accurate staging based on lymph node involvement before treatment plays an integral part in planning further medical, surgical, and/or radiation interventions. We believe that the results obtained to date are very promising, and support OCT as a potentially cost-effective technique that could allow lymph node assessment in situ without having to physically resect and histologically process the tissue, as well as reduce potential morbid complications like lymphedema.

Three-dimensional transcapsule imaging of lymph nodes and nodal micro-architecture demonstrate the potential of OCT for the intraoperative evaluation of lymph nodes where it may no longer be necessary to remove lymph nodes for postoperative assessment and cancer staging. OCT in combination with current lymph node mapping procedures could provide surgeons with a technology for future real-time intraoperative evaluation and staging of cancer in situ, using handheld surgical probes.[30,31] Although OCT provides high-resolution images, it is at the expense of imaging penetration, which is less than other imaging modalities such as X-ray, MRI, PET, or ultrasound imaging, but still greater than other optical techniques such as bright-field, confocal, or multiphoton microscopy. The imaging depth penetration limits of OCT imaging is typically only 1–3 mm, depending on the optical properties of the tissue. Needlebased OCT probes, which could be inserted into lymph nodes either transcutaneously or during open surgical procedures, would allow the surgeon to image into deeper, unexposed lymph nodes.[32,33]

The data from this study therefore support the future investigation of a handheld surgical probe capable of in situ lymph node imaging and cancer staging, as well as needlebased probes that would be inserted into lymph nodes, allowing the surgeon to image deeper into the unexposed areas.

ACKNOWLEDGMENT

Stephen Boppart is co-founder and chief medical officer of Diagnostic Photonics Inc., which is commercializing Interferometric Synthetic Aperture Microscopy for intraoperative tumor margin assessment. He also receives royalties from patents licensed by the Massachusetts Institute of Technology related to OCT. This research was supported in part by grants from the National Institutes of Health NIBIB, R01 EB012479, and NIBIB, R01 EB013723 (S.A.B.). The authors thank Darold Spillman for his assistance with project coordination and information technology management, and Freddy T. Nguyen for helpful discussions and technical support during the experimental studies. Additional information can be found at http://biophotonics.illinois.edu.

REFERENCES

1. Willard-Mack CL. Normal structure, function, and histology of lymph nodes. Toxicol Pathol. 2006; 34:409–424. [PubMed: 17067937]
2. Torabi M, Aquino SL, Harisinghani MG. Current concepts in lymph node imaging. J Nucl Med. 2004; 45:1509–1518. [PubMed: 15347718]
3. Gadd M. Sentinel lymph node biopsy for staging early breast cancer: minimizing the trade-off by maximizing the accuracy. Ann Oncol. 2009; 20:973–975. [PubMed: 19465427]
4. Quan ML, McCready D. The evolution of lymph node assessment in breast cancer. J Surg Oncol. 2009; 99:194–198. [PubMed: 19021226]
5. Szabo BK, Aspelin P, Kristoffersen WM, Tot T, Bone B. Invasive breast cancer: correlation of dynamic mr features with prognostic factors. Eur Radiol. 2003; 13:2425–2435. [PubMed: 12898176]
6. Fischbein NJ, Noworolski SM, Henry RG, Kaplan MJ, Dillon WP, Nelson SJ. Assessment of metastatic cervical adenopathy using dynamic contrast-enhanced MR imaging. Am J Neuroradiol. 2003; 24:301–311. [PubMed: 12637272]
7. Kim SH, Kim SC, Choi BI, Han MC. Uterine cervical carcinoma: evaluation of pelvic lymph node metastasis with MR imaging. Radiology. 1994; 190:807–811. [PubMed: 8115631]
8. Harisinghani MG, Barentsz J, Hahn PF, et al. Noninvasive detection of clinically occult lymph node metastases in prostate cancer. N Engl J Med. 2003; 348:2491–2499. [PubMed: 12815134]
9. Anzai Y, Blackwell KE, Hirschowitz SL, et al. Initial clinical experience with dextran-coated superparamagnetic iron oxide for detection of lymph node metastases in patients with head and neck cancer. Radiology. 1994; 192:709–715. [PubMed: 7520182]
10. Krag D, Weaver D, Ashikaga T, et al. The sentinel node in breast cancer—a multicenter validation study. N Engl J Med. 1998; 339:941–946. [PubMed: 9753708]
11. Blessing WD, Stolier AJ, Teng SC, Bolton JS, Fuhrman GM. A comparison of methylene blue and lymphazurin in breast cancer sentinel node mapping. Am J Surg. 2002; 184:341–345. [PubMed: 12383897]
12. Schaafsma BE, Mieog JS, Hutteman M, et al. The clinical use of indocyanine green as a near-infrared fluorescent contrast agent for image-guided oncologic surgery. J Surg Oncol. 2011; 104:323–332. [PubMed: 21495033]
13. Sampath L, Wang W, Sevick-Muraca EM. Near-infrared fluorescent optical imaging for nodal staging. J Biomed Opt. 2008; 13:041312. [PubMed: 19021320]
14. Rosbach KJ, Shin D, Muldoon TJ, et al. High-resolution fiber optic microscopy with fluorescent contrast enhancement for the identification of axillary lymph node metastases in breast cancer: a pilot study. Biomed Opt Express. 2010; 1:911–922. [PubMed: 21258518]
15. Nguyen NQ, Biankin AV, Leong RW, et al. Real time intraoperative confocal laser microscopy-guided surgery. Ann Surg. 2009; 249:735–737. [PubMed: 19387332]
16. Fujimoto JG, Brezinski ME, Tearney GJ, et al. Optical biopsy and imaging using optical coherence tomography. Nat Med. 1995; 1:970–972. [PubMed: 7585229]
17. Tearney GJ, Brezinski ME, Bouma BE, Boppart SA, Pitris C, Southern JF, Fujimoto JG. In vivo endoscopic optical biopsy with optical coherence tomography. Science. 1997; 276:2037–2039. [PubMed: 9197265]
18. Boppart SA, Bouma BE, Pitris C, Southern JF, Brezinski ME, Fujimoto JG. *In vivo* cellular optical coherence tomography imaging. Nat Med. 1998; 4:861–865. [PubMed: 9662382]

19. Brezinski ME, Tearney GJ, Boppart SA, Swanson EA, Southern JF, Fujimoto JG. Optical biopsy with optical coherence tomography: feasibility for surgical diagnostics. J Surg Res. 1997; 71:32–40. [PubMed: 9271275]
20. Boppart SA, Herrmann JM, Pitris C, Stamper DL, Brezinski ME, Fujimoto JG. High-resolution optical coherence tomography guided laser ablation of surgical tissue. J Surg Res. 1999; 82:275–284. [PubMed: 10090840]
21. Boppart SA, Bouma BE, Pitris C, Tearney GJ, Southern JF, Brezinski ME, Fujimoto JG. Intraoperative assessment of microsurgery with three-dimensional optical coherence tomography. Radiology. 1998; 208:81–86. [PubMed: 9646796]
22. Nguyen FT, Zysk AM, Chaney EJ, et al. Intraoperative evaluation of breast tumor margins with optical coherence tomography. Cancer Res. 2009; 69:8790–8796. [PubMed: 19910294]
23. Luo W, Nguyen FT, Zysk AM, et al. Optical biopsy of lymph node morphology using optical coherence tomography. Tech Cancer Res Treat. 2005; 4:539–547.
24. McLaughlin RA, Scolaro L, Robbins P, Hamza S, Saunders C, Sampson DD. Imaging of human lymph nodes using optical coherence tomography: potential for staging cancer. Cancer Res. 2010; 70:2579–2584. [PubMed: 20233873]
25. Nguyen FT, Zysk AM, Chaney EJ, et al. Optical coherence tomography: the intraoperative assessment of lymph nodes in breast cancer. IEEE Eng Med Biol. 2010; 29:63–70.
26. Taback B, Hashimoto K, Kuo CT, Chan A, Giuliano AE, Hoon DS. Molecular lymphatic mapping of the sentinel lymph node. Am J Pathol. 2002; 161:1153–1161. [PubMed: 12368189]
27. Klein T, Wieser W, Eigenwillig CM, Biedermann BR, Huber R. Megahertz OCT for ultrawide-field retinal imaging with a 1050 nm Fourier domain mode-locked laser. Opt Express. 2011; 19:3044–3062. [PubMed: 21369128]
28. Tsai TH, Zhou C, Adler DC, Fujimoto JG. Frequency comb swept lasers. Opt Express. 2009; 17:21257–21270. [PubMed: 19997365]
29. de Boer M, van Deurzen CHM, van Dijck JAAM, et al. Micrometastases or isolated tumor cells and the outcome of breast cancer. N Engl J Med. 2009; 361:653–663. [PubMed: 19675329]
30. Boppart SA, Bouma BE, Pitris C, Tearney GJ, Brezinski ME, Fujimoto JG. Forward-imaging instruments for optical coherence tomographic imaging. Opt Lett. 1997; 22:1618–1620. [PubMed: 18188315]
31. Jung W, Kim J, Jeon M, Chaney EJ, Stewart CJ, Boppart SA. Handheld optical coherence tomography scanner for primary care diagnostics. IEEE Trans Biomed Eng. 2011; 58:741–744. [PubMed: 21134801]
32. Zysk AM, Nguyen FT, Chaney EJ, et al. Clinical feasibility of microscopically-guided breast needle biopsy using a fiber optic probe with computer-aided detection. Tech Cancer Res Treat. 2009; 8:315–322.
33. Li X, Chudoba C, Ko T, Pitris C, Fujimoto JG. Imaging needle for optical coherence tomography. Opt Lett. 2000; 25:1520–1522. [PubMed: 18066265]

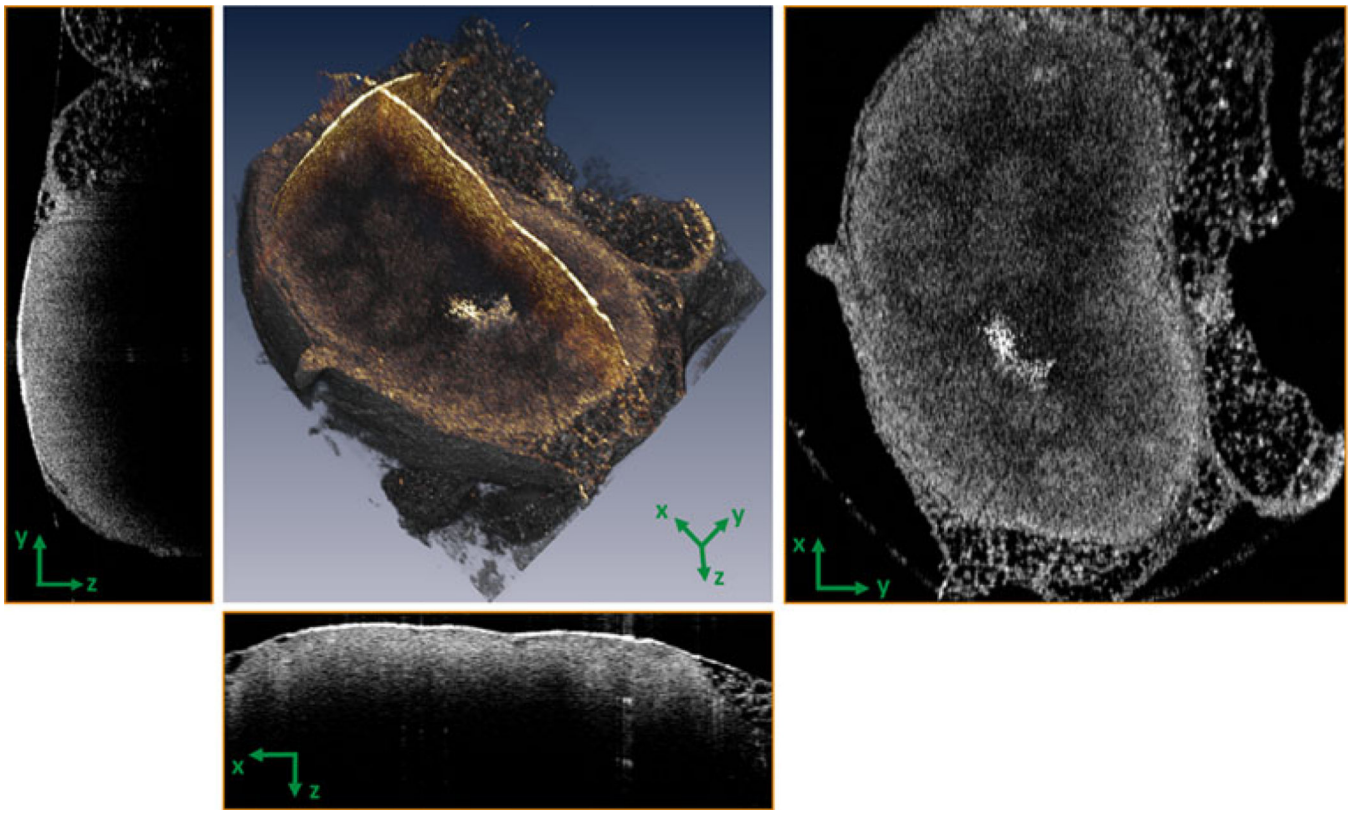

FIG. 1.

Three-dimensional OCT of a normal lymph node. Cross-sectional (*y–z* and *x–z*) and *en face* (*x–y*) images can be computationally extracted from the highly sampled 3-D data volumes as shown here, and in subsequent figures

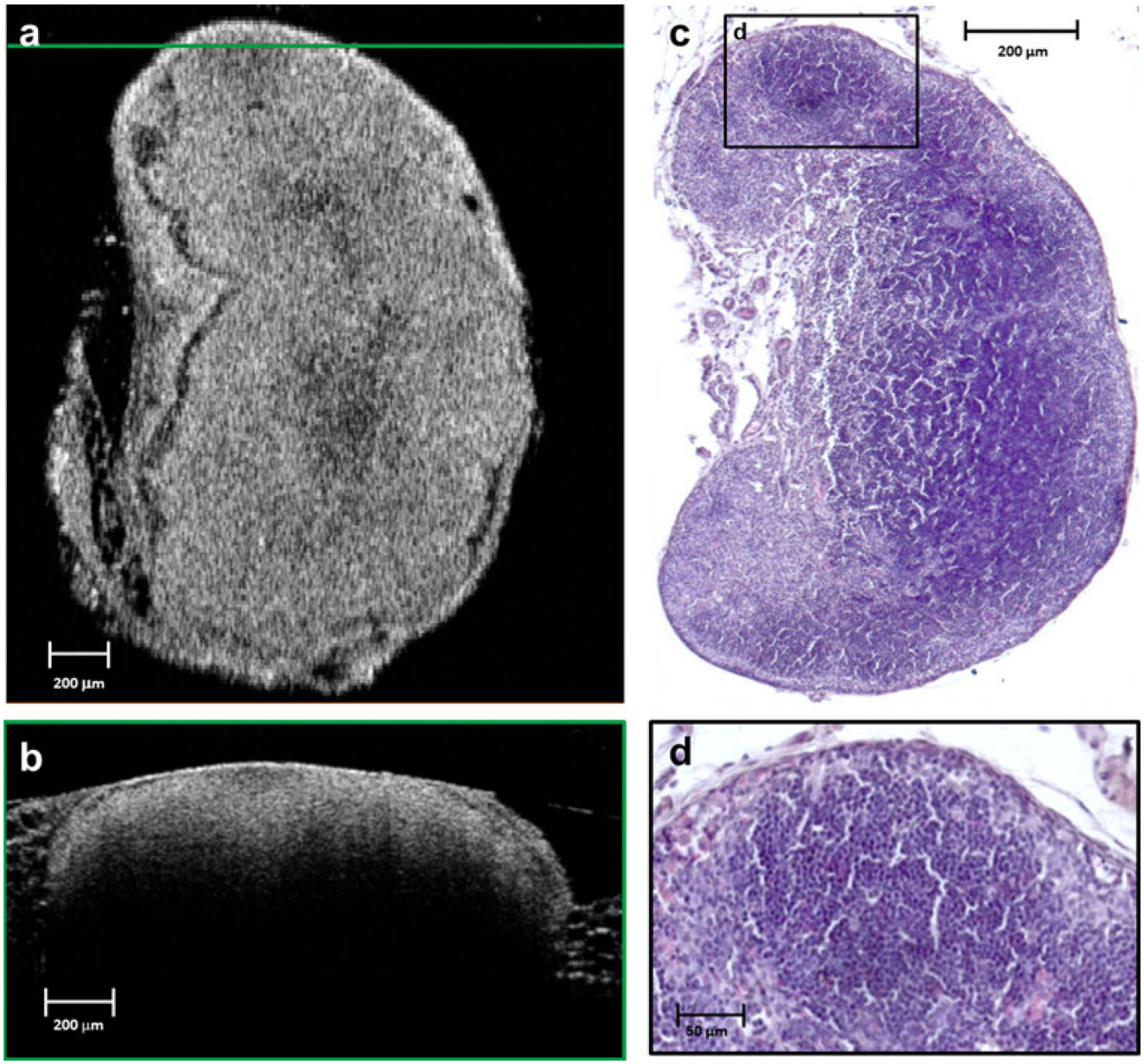

FIG. 2.

Normal lymph node (day 0). An *en face* OCT image plane (**a**) is matched to the corresponding histological section (**c**). *The horizontal green line* in (**a**) indicates the location of the cross-sectional OCT image in (**b**). The *black-framed region* in the histological section (**c**) is magnified in (**d**) to highlight a follicle and other structural features of the normal lymph node

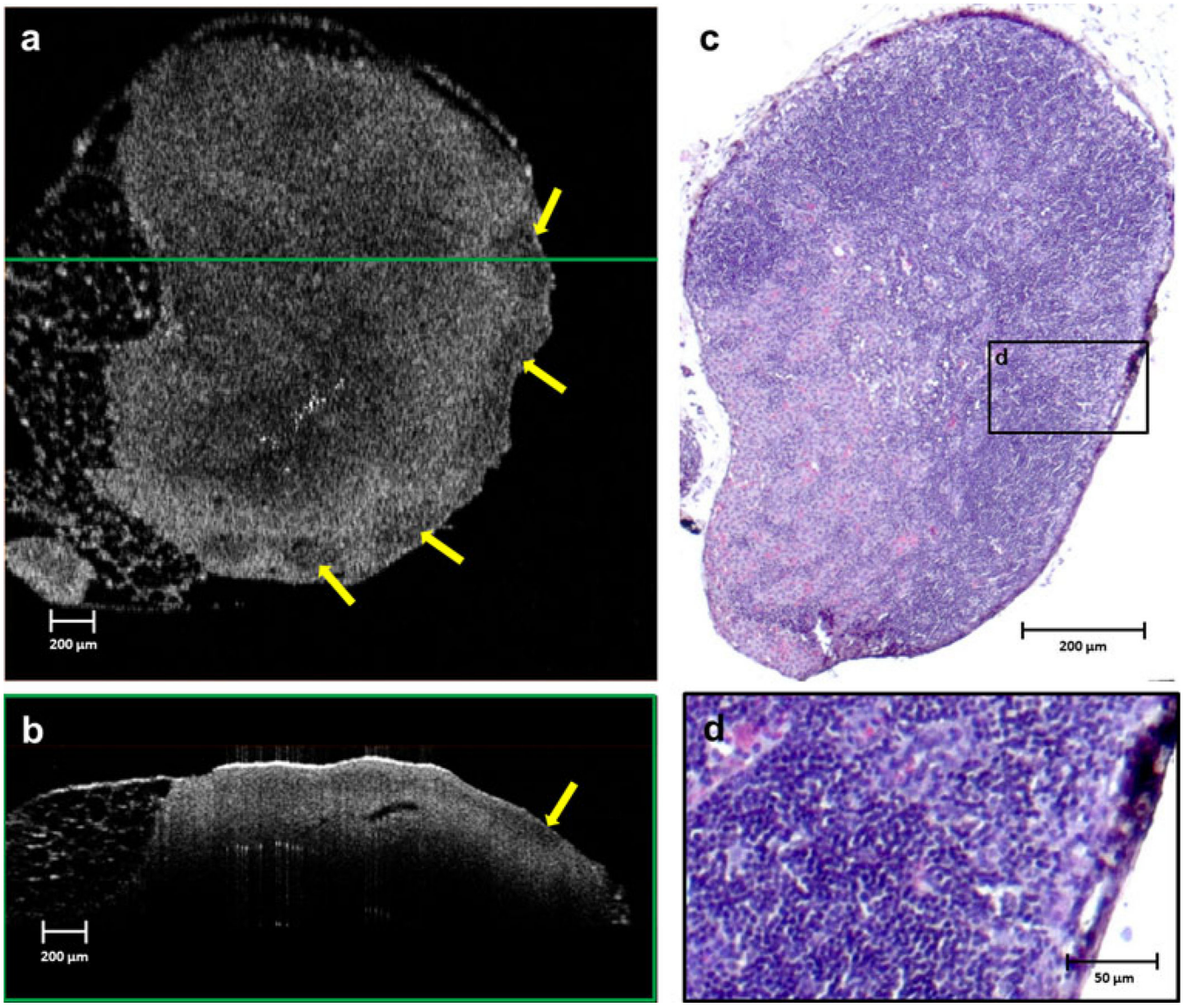

FIG. 3.

Popliteal lymph node imaged on day 3 after injection of tumor cells in the footpad of a preclinical rat metastatic tumor model. An *en face* OCT image is shown in (**a**). The cross-sectional OCT image in (**b**) was extracted at the position indicated by the *horizontal green line* on the *en face* OCT image in (**a**). The capsular structure is less distinct, and mild inflammation results in regions of lower optical scattering in the subcapsular region (*yellow arrows*). The histological section corresponding to the *en face* OCT image in (**a**) is shown in (**c**). Similar inflammation-related features are clearly visible on high magnification (**d**) of the area indicated by the *black frame* in the histology section (**c**)

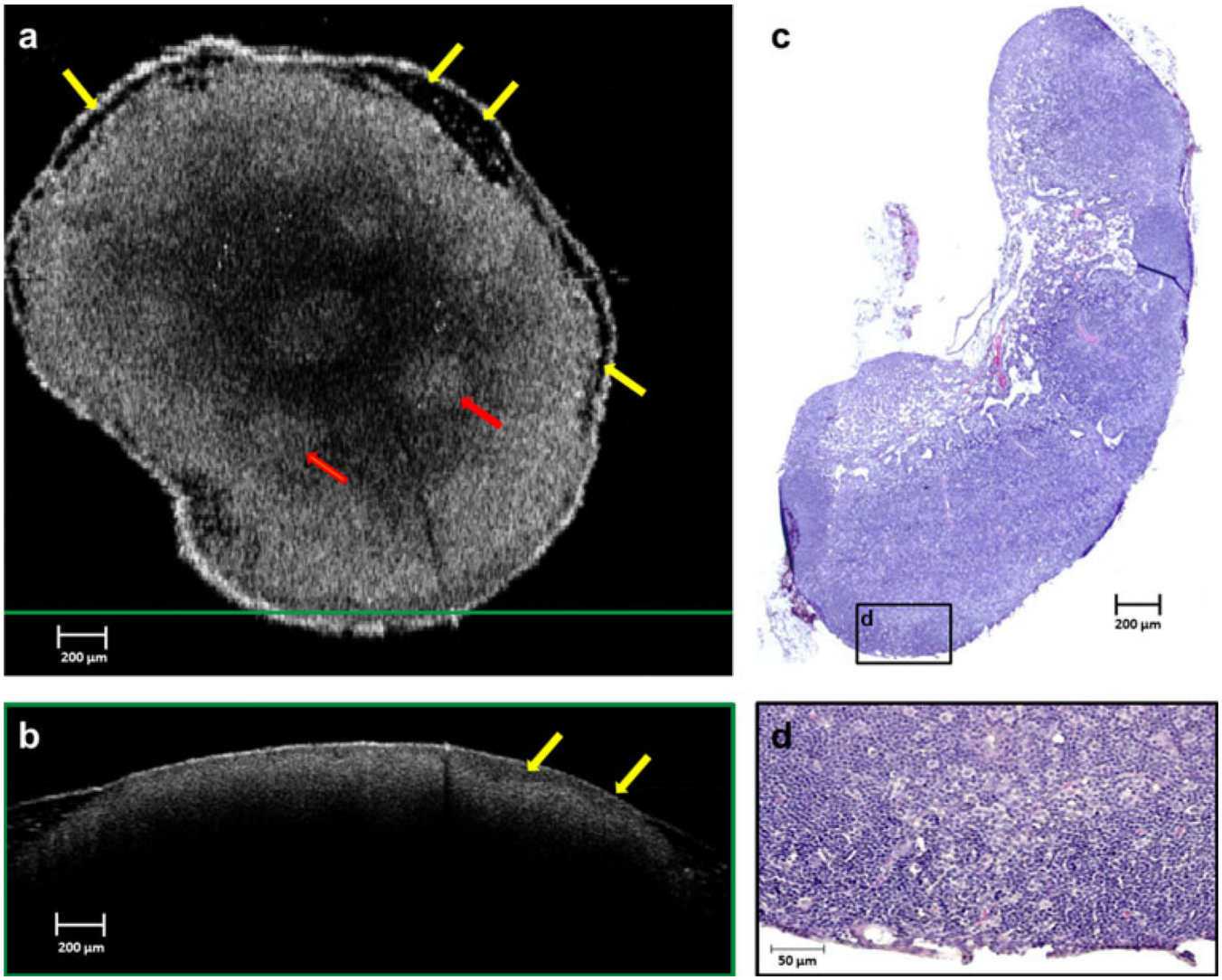

FIG. 4.

Lymph node imaged on day 5 after injection. A new heterogeneous low-scattering layer (*yellow arrows*) in the capsular and subcapsular region is prominent in both the *en face* (**a**) and cross-sectional (**b**) OCT images, and focal regions of higher scattering have become evident in the cortex (*red arrows*). The histological section corresponding to the *en face* OCT image is shown in (**c**). Infiltration of tumor cells and macrophages into the precortical region is visible in the magnified area (**d**) from the *black-framed region* shown on the histology section in (**c**)

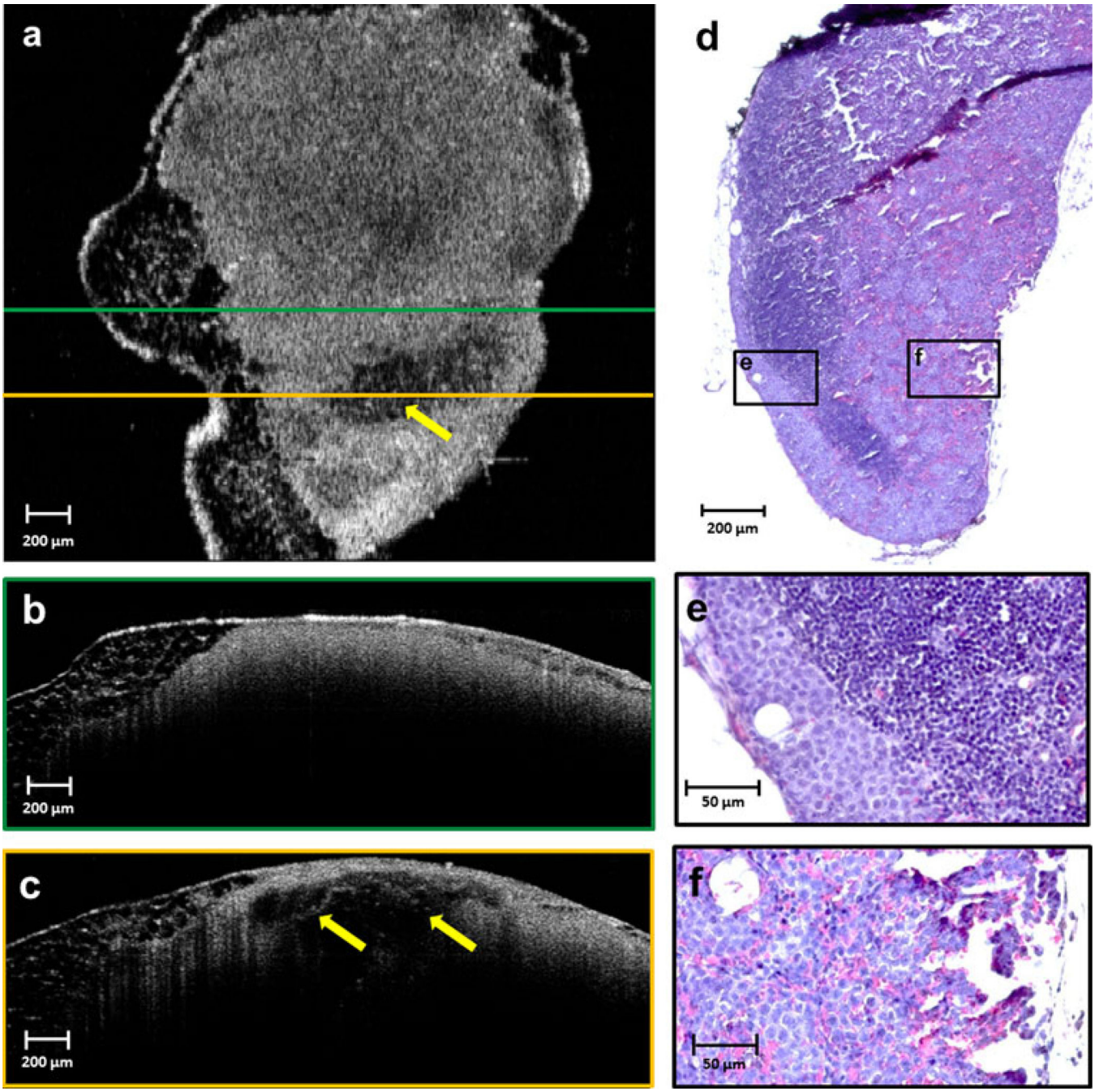

FIG. 5.

Lymph node imaged on day 7 after injection. An *en face* OCT (**a**) and corresponding histology image (**d**) are shown. Lowscattering subcapsular regions have extended deeper into the node, and a more homogeneous highly scattering cortex is evident, as shown in (**b**), where follicular structures are no longer visible, as confirmed by histology in (**e**). An adjacent area reveals decreased optical scattering (*yellow arrows*), as seen in (**c**), from a histologically verified region of inflammation with aggregates of macrophages but no tumor cells (**f**). The green and *yellow frames* around the crosssectional OCT images (**b** and c,

respectively) correspond to the horizontal lines of the same color in (**a**), indicating the positions of these cross sections relative to the *en face* OCT image. The highlighted and magnified histology areas (**e** and **f**) correspond to the left and right black-framed areas, respectively, on the complete *en face* lymph node section in (**d**)

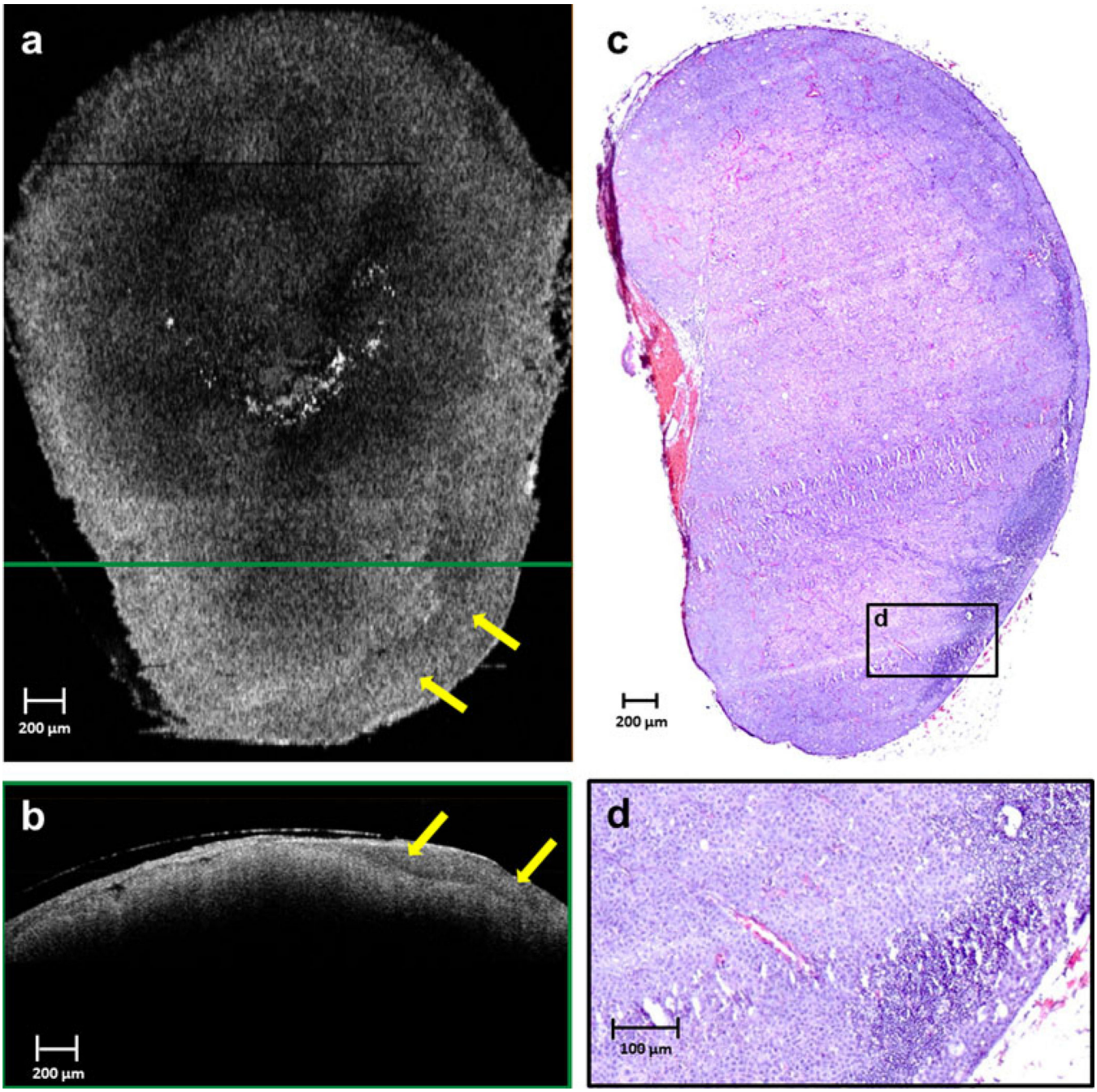

FIG. 6.

Lymph node imaged on day 9 after injection. OCT reveals a relatively homogeneous scattering pattern across the lymph node in both *en face* (**a**) and cross-sectional (**b**) images, due to near-total effacement of normal nodal architecture, as shown in the corresponding histological section in (**c**). A thick low-scattering layer in the capsular and subcapsular region (*yellow arrows*) can be seen in the *en face* (**a**) and cross-sectional (**b**) OCT images, resulting from metastatic tumor invasion. This correlates to regions in the histology that show only few remaining lymphocytes in the node (**d**). The *green-framed* cross-sectional

OCT image in **(b)** was extracted from the location of the *horizontal green line shown on the en face* imaging in (**a**). The magnified histological region in (**d**) is from the *black-framed region* in (**c**)